DOI: 10.24427/978-83-67185-12-7_1

Chapter 1
The influence of reinforcement on the distribution of electric field intensity

Agnieszka Choroszucho
Bialystok University of Technology, Faculty of Electrical Engineering

Abstract: The aim of this paper is to analyze the distribution of a high frequency electromagnetic field (f = 2.4 GHz) inside the living room. The influence of the building material and the diameter of reinforcement on the distribution of the electromagnetic field was shown. The finite-difference time-domain method (FDTD) was used for analysis. The results prove that mounting transmitters on walls with no reinforcement enables an even distribution of the electromagnetic field. The diameter of the rods influences merely the distribution of the field and its value only at a distance of 4 m. A detailed analysis of influence of the type of building construction will make it possible to solve the problem connected with fading.

Keywords: wireless communication systems, electromagnetic wave propagation, building materials, finite difference time domain method (FDTD).

Introduction

The rapid development of radio communication systems enforces the use of electromagnetic waves at constantly increasing frequencies. Their use in, among others, radiolocation, radio communications and satellite communication causes a number of transmitters to grow exponentially [1, 11]. With higher frequencies this growth is more dynamic due to the introduction of wireless communication. The analysis of wave propagation at high frequencies entails the necessity to research the phenomenon connected with the effects that electromagnetic fields have in interaction with materials of different properties. The use of modern-day systems of wireless communication requires taking into account these effects which may lower the effectiveness of data transmission. Such phenomena as diffraction or interference are the subject of various research which aim to determine the distribution of the field's intensity in the discussed settings as precisely as possible. The analysis of fields used in wireless communication systems also requires considering the effects connected

with multiple refractions, deflections and damping of waves in areas of different material construction. The mentioned effects are a direct result of wave propagation in structures containing metal elements or constructed of non-ideal dielectrics. They contain complex settings, with periodic structures and singular, non-typical elements with unique material properties and non-typical geometry. Such situations require including resistance of the wireless communication channel to disruptions, interference from neighboring base units, signal delays, periodic damping and loss of signal. Some of these factors are random occurrences, connected with changes in the conditions of wave propagation. However, the construction of a resistant and reliable wireless communication network requires including all the known factors that influence field distribution as early as in the design stages (geometry and construction of buildings, complex material structures in the path between the signal emitter and the base unit etc.). The mentioned problems are especially visible in low range wireless networks (Wi-Fi), used in buildings. Taking into account the construction of both new and already existing buildings influences the location of signal units [13]. The analysis of the field's distribution done in such a way allows to determine the minimal value of the base unit's power, which will enable constant connectivity between the base and mobile appliances. However, these ranges are generalized and have a wide span, for example at 900 MHz frequency, and the damping of the building has values from 37dB to –8dB [1].

The aim of this research is to determine the distribution of the EM field in constructions made of concrete, including various sizes of reinforcement. The results will allow in the future to solve problems connected with signal loss and design optimal locations of a field source within complex reinforced constructions. The article presents the analysis of the properties of materials used in constructing accommodation spaces.

Mathematical model (FDTD)

To determine the distribution of the EM field in the analyzed settings, the finite difference time domain method (FDTD) was used [10]. The method is based on Maxwell's curl equations in time and space:

$$\nabla \times \vec{E} = -\mu \frac{\partial \vec{H}}{\partial t}, \tag{1.1}$$

$$\nabla \times \vec{H} = \sigma \vec{E} + \varepsilon \frac{\partial \vec{E}}{\partial t}, \tag{1.2}$$

which are then transformed into their differentia form. The equations are solved simultaneously in time and space.

The FDTD method allows the analysis of complex structures, in which every material has a corresponding material property, which directly influences the correctness of the results. In order to obtain a simultaneous scalar equation describing individual components of the field, the equations (1)–(2) are subjected to decomposition in the Cartesian coordinate system. As an example, the equation for the EM field intensity component (E_z) in its scalar form is:

$$\frac{\partial E_z}{\partial t} = \frac{1}{\varepsilon}\left(\frac{\partial H_y}{\partial x} - \frac{\partial H_x}{\partial y} - \sigma E_z\right). \tag{1.3}$$

With three-dimensional issues, in a classic formulation of the method, the Yee cell is used (Fig. 1.1) [2]. It contains six appropriately placed component vectors of field intensity: electrical (E_x, E_y, E_z) and magnetic (H_x, H_y, H_z). The use of the FDTD method is based on the division of the whole analyzed area into an appropriate number of cells.

The difference schematic in the area is realized through the proper distribution of component vectors of intensity of the electrical **E** and magnetic field **H** within each cell (Fig. 1.1). The components of the EM field are calculated at a different point in space. The vectors E_x, E_y, E_z associated with the Yee cell are anchored in mid-points of appropriate edges, and the H_x, H_y, H_z vectors – in the middle of the planes forming the sides of the cell. Appropriate component intensity vectors of the magnetic field circulating around it surround each component intensity vector of the electrical field. In the case of component intensity vectors of the magnetic field the presentation is analogical.

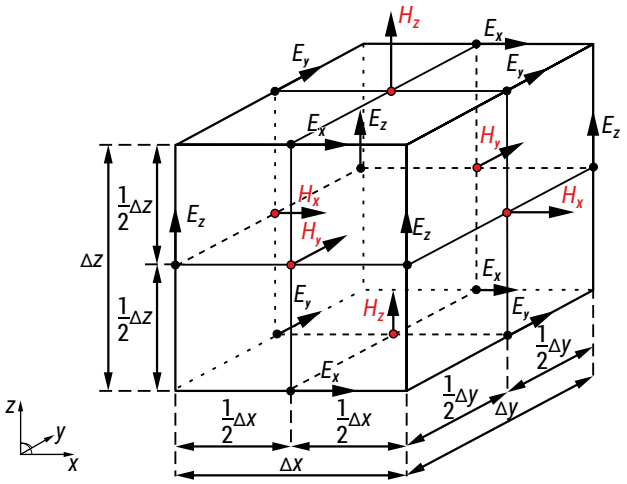

FIGURE 1.1. A single Yee cell in the FDTD method

The integration of Maxwell equations in time is based on using the two-step schematic. In selected moments in time, in which the distribution of the electrical field is determined, the compound vector values of the intensity of the magnetic

field are moved in time by $\Delta t/2$ in relevance to them. The determining of compound intensity vectors of the electrical field E_x, E_y, E_z is possible with the prior calculation of the compound intensity vectors of the magnetic field H_x, H_y, H_z in the previous time step of the algorithm. Using the already calculated values H_x, H_y, H_z, the next values of the compound vectors of the electric field are determined E_x, E_y, E_z. The described series of steps is called the time jump process (Fig. 1.2).

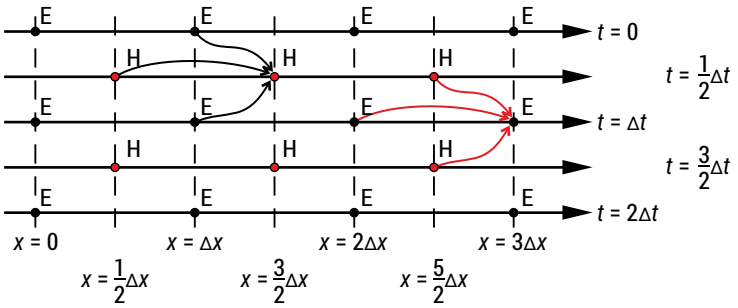

FIGURE 1.2. Calculating the values of electric and magnetic fields' intensity in the FDTD algorithm

Another advantage of the algorithm is the assumption that the size of the Yee cell is determined by growth in the Δ space. In a three-dimensional case, if assumed that the Yee cell is a cube, where $\Delta = \Delta x = \Delta y = \Delta z$, then the distances between the appropriate intensity compounds of the electrical and magnetic field are 0.5Δ. Depending on the calculation requirements, the elementary Yee cell after previous modification of difference equations may be cuboid in shape, where $\Delta x^1 \Delta y^1 \Delta z$.

As a result of the approximation of partial derivatives, the Maxwell equation is acquired in a difference form. Therefore, the equation (3) is:

$$\frac{{}^{n+1}_{i,j,k}E_z - {}^{n}_{i,j,k}E_z}{\Delta_t} = \frac{1}{\varepsilon_{i,j,k}} \left(\frac{{}^{n+\frac{1}{2}}_{i+\frac{1}{2},j,k}H_y - {}^{n+\frac{1}{2}}_{i-\frac{1}{2},j,k}H_y}{\Delta_x} - \frac{{}^{n+\frac{1}{2}}_{i,j+\frac{1}{2},k}H_x - {}^{n+\frac{1}{2}}_{i,j-\frac{1}{2},k}H_x}{\Delta_y} - \sigma_{i,j,k}\, {}^{n+\frac{1}{2}}_{i,j,k}E_z \right), \tag{1.4}$$

which after transformations allows to determine the compound value along the x axis of the electrical field's intensity at the point of observation (i, j+1/2, k+1/2) in time (n+1/2), based on the calculated compounds of the electromagnetic field in the previous moments t, at appropriate points in space [14].

Due to the simple formulation of the method and easy imaging of the geometry of the analyzed set, it is especially useful in calculating electromagnetic fields changing in time, in the range of high frequencies and broadband signals.

Numerical analysis

The distribution of the electromagnetic field in rooms containing concrete elements was determined, and introduced without changes in geometry reinforcement in supporting walls (top and left) and the post (in Fig. 1.3 marked in grey). In order to compare the effect of reinforcement on the distribution of the electromagnetic field, different diameters of reinforcing rods were analyzed.

The first model (M1) was created from concrete constructs with no reinforcement according to the existing design (Figs. 1.3, 1.4).

In order to compare the distribution of the electromagnetic field with the inclusion of refractions from rods in the top and left wall and the post, M2 was designed. The top element of 3.2 m in length consisted of: 4 rods running lengthwise with Φ = 8 mm and a concrete cover of 20 mm and rods placed every 200 mm with two rows of 16 vertical rods on either side of the wall (Φ = 8 mm), spaced every 200 mm and a concrete cover of 20 mm (including the starting distance of 40 mm) and two rows of anchoring loops with 16 horizontal rods connecting the vertical rods (Φ = 8 mm) at a height of 200 and 400 mm, spaced every 200 mm (Fig. 5).

Another reinforced element was the left wall of 4.9 m in length: 4 rods running lengthwise (Φ = 8 mm) with concrete thickness of 20 mm (from the outside edge to the reinforcement), spaced every 200 mm, two rows of 25 vertical rods Φ = 8 mm on either side of the wall spaced every 200 mm and a concrete cover of 20 mm (including the starting distance of 40 mm), two rows of anchor loops of 25 horizontal rods Φ = 8 mm connecting the vertical rods at the same height and spaced as in the top wall (Fig. 1.3).

Additionally, within the post there was introduced reinforcement of eight vertical rods Φ = 20 mm in diameter with concrete cover of 40 mm and 5 stirrups Φ = 8 mm spaced every 100 mm, including the distance from the ground of 50 mm (Figs. 1.3, 1.4).

The third model (M3) was based on the construction of M2 with modifications to the rods' diameter (from Φ = 8 to Φ = 12 mm). The post construction remained unchanged.

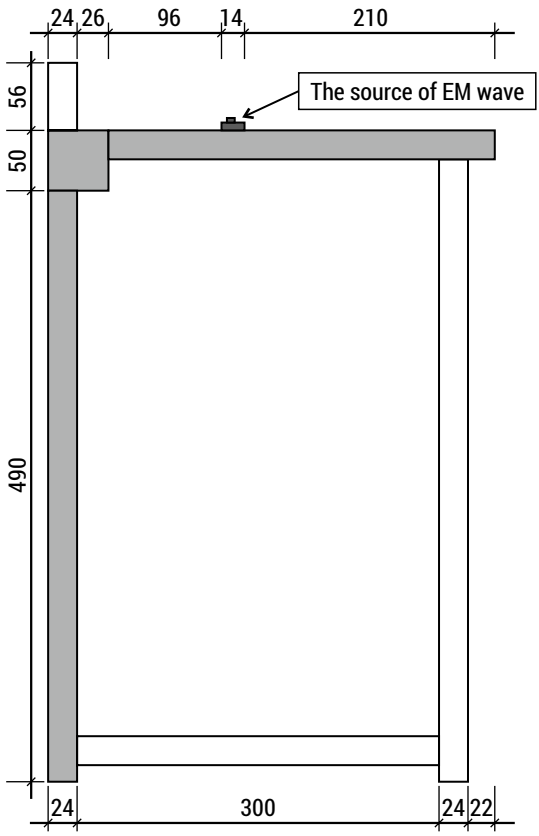

FIGURE 1.3. Geometry of the analyzed room (dimensions in cm)

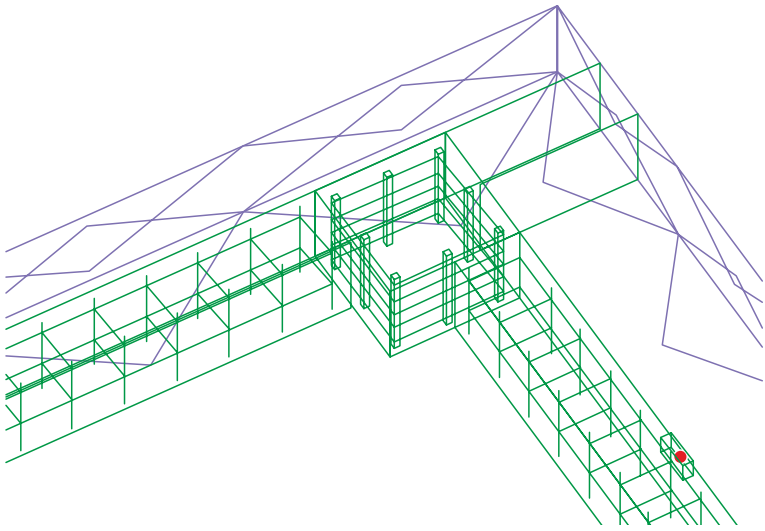

FIGURE 1.4. Reinforcement in the post, top and left wall with absorption conditions

An important topic with the numerical methods is stability. An appropriate choice of parameters of the difference schematic (in time Δt and space Δx, Δy, Δz) is decisive in the stability of the FDTD method, as well as the preciseness of the solutions. The Courant-Friedrichs-Lewy (CFL) condition determines dependency between the minimal value of a time step Δt and the biggest size of the Yee cell (Δx, Δy, Δz) [9, 10]. The stability criterion for a three-dimensional Yee cell is described with the following equation:

$$\Delta t \leq \frac{1}{c_0 \sqrt{\frac{1}{(\Delta x)^2} + \frac{1}{(\Delta y)^2} + \frac{1}{(\Delta z)^2}}} \tag{1.5}$$

In the FDTD algorithm the presented criterion is fulfilled on the condition that the spreading speed of the disturbance (change of field value) is greater or equal to the speed of the wave.

An important factor is the correct recreation of the intended signal. In order to eliminate such mistakes, the Nyquist criterion is used [3, 4, 6]. In practice, it is assumed that the biggest step in space (Δx, Δy, Δz) should be at least ten times smaller than the length of the wave λ [6]:

$$\max(\Delta x, \Delta y, \Delta z) \leq \lambda / 10. \tag{1.6}$$

In the analyzed sets, the source of the signal was a dipole generating a harmonic wave with the frequency of 2.4 GHz. The condition (6) has been fulfilled because a net of cubic elements 10′10′10 mm was assumed.

When solving this type of tasks, it is necessary to limit the area of analysis. Boundary conditions properly represent physical effects at the edges of the analyzed area and are necessary for the numerical solution of field tasks. In the discussed sets, Mur's absorption conditions of the first order were used [4, 5].

The conducted calculations analyzed only the influence of the used building material and reinforcement on the distribution of the field in a given room. Relating to the above statement, refractions and reflections of the EM wave from the ceiling were not taken into account. Absorption conditions were used also on its top and bottom surfaces. The size of the analyzed numerical model was approximately composed of 4 612 416 Yee cells.

All elements of the construction had material data of standard concrete assigned to them. The permittivity was assumed at $\varepsilon_r = 5$ and conductivity at $\sigma = 0.04$ S/m. At the height of 2 m on the outside of the top wall there was a cuboid of dielectric parameters: $\varepsilon_r = 2.2$, $\mu_r = 1$, on which a transmitter was placed, emitting a sinusoidal signal of a frequency $f = 2.4$ GHz and amplitude of 1.

Results of the analysis

The assessment of the distribution of the EM field was obtained by using the FDTD method. A comparison of the distribution of the EM field in a fixed state and for a given time step was made.

In Fig. 1.5 the distribution of the EM field was presented inside the analyzed construct made only of concrete. The transfer of the wave through the dielectric (concrete) causes a decrease in the EM field's value. Part of the wave becomes damped by passing through a different medium and reflected multiple times inside the wall, and part of it becomes reflected on the air-dielectric boundary. When comparing the distribution of the EM field in the three analyzed cases, it is visible that the wave spreads more evenly in constructs with no reinforcement both in front of and behind the wall (Figs. 1.5–1.7). In the models with steel rods there are unevenly spreading, numerous shadow zones in the immediate proximity to the wall. Also, reflections of the wave from the rods cause multiple interferences with visible deviations from the even distribution of signal. The amassing of interference within the room (taking into account reflections from all the walls) generally decreases the value of the compound number E_z and the average distribution of the field, which has similar values to the non-reinforced scenario only at a distance of 4 m from the signal source.

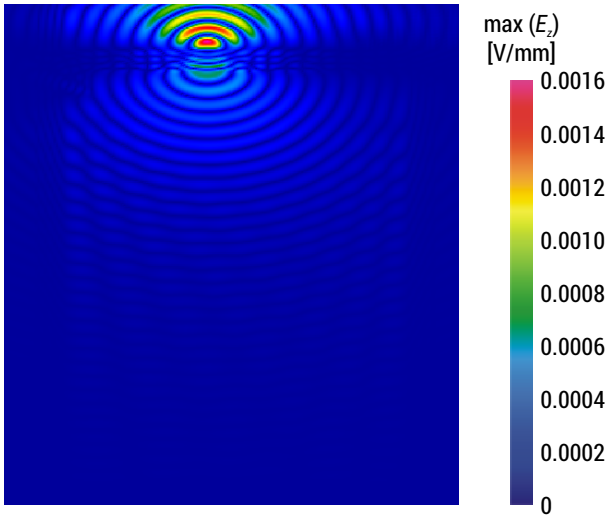

FIGURE 1.5. Reinforcement in the post, top and left wall with absorption conditions (M1)

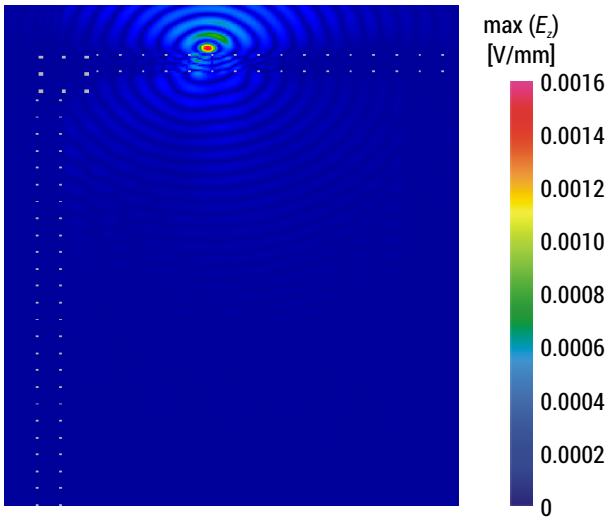

FIGURE 1.6. Distribution of EM field inside a room with reinforcement Φ = 8 mm (M2)

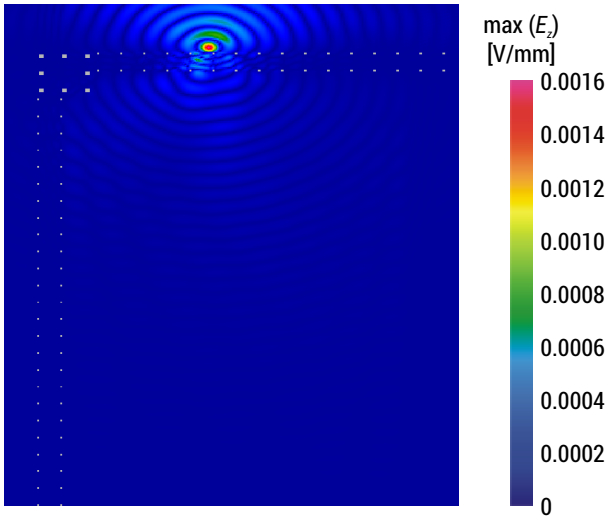

FIGURE 1.7. Distribution of EM field inside a room with reinforcement Φ = 12 mm (M3)

The phenomenon of reflection from the walls causes temporary increases in the field's value inside the room. The concrete post construction introduces additional reflections, and the reinforcement within the post participates in the creation of complex processes: reflections on the air-post boundary and the reinforcement-concrete boundary, where multiple reflections take place. The mentioned phenomenon causes an increase in the signal strength, as well as temporary fading in the area close to the reinforced construction (up to 1 m). In the construction with iron rods of 12 mm diameter (M3) the value of the EM field inside the room is comparable

with the Φ = 8 mm model (M2). The increase in reinforcement diameter causes only local decreasing of the compound E_z value in areas of the rods and a larger area of the shadow zone (Fig. 1.7). Reinforcement causes a non-uniform distribution of field value and decreasing the compound E_z value by 10–20% on average, in comparison with the model with no reinforcement (Figs. 1.5–1.7).

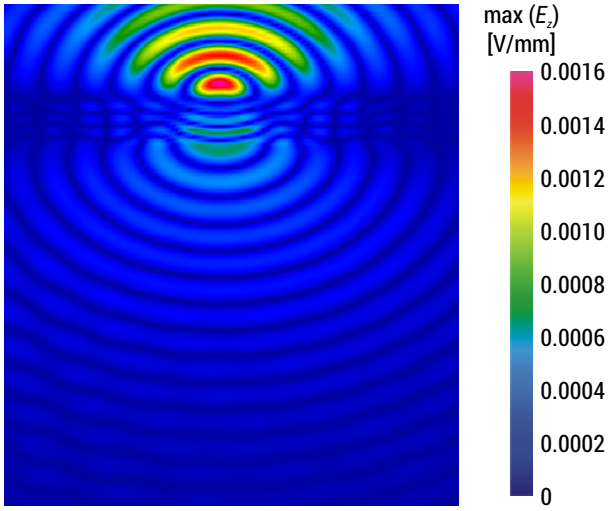

FIGURE 1.8. Proximity zone containing a point source of the field (model composed of only concrete – M1)

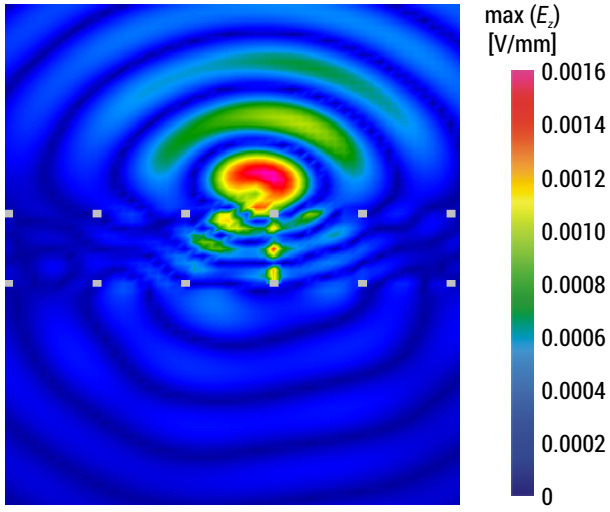

FIGURE 1.9. Proximity zone containing a point source of the field. Model composed of concrete with reinforcements: Φ = 8 mm (M2)

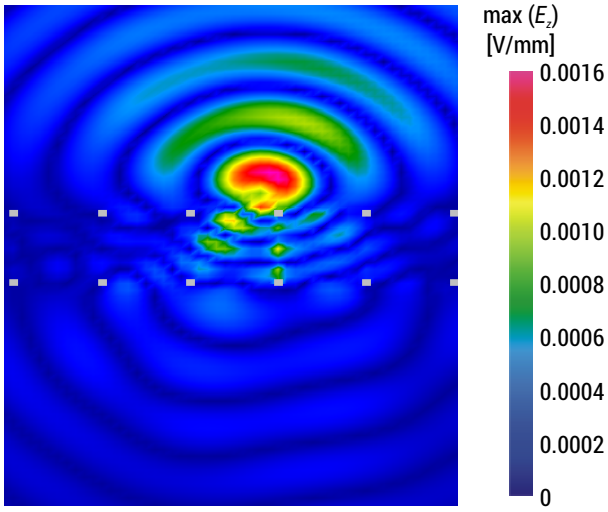

FIGURE 1.10. Proximity zone containing a point source of the field. Model composed of concrete with reinforcements: Φ = 12 mm (M3)

The increase of areas in the proximity to the point source of the field is illustrated in Figs. 1.7–1.9. Clearly visible are the refractions of the EM wave at the air-concrete boundary causing decrease in signal strength, decrease in wavelength and a localized change in the direction of wave propagation. Thicker reinforcement would cause larger areas of signal fading, whereas with appropriately chosen rod diameters and their spacing it would be possible to analyze the issues of screening.

Conclusions

In material mediums the speed of the EM wave is always smaller and depends on the material and frequency. Small non-uniformities of the field cause the wave to partially scatter practically in all directions.

There are many problems with generating and radiating higher levels of power. The analysis of large systems requires consideration of the future application of homogenization of structures in terms of material data in order to, for example, reduce calculation costs related to the reduction of the mesh and obtain more accurate results. The results show that mounting transmitters on walls without reinforcement significantly improves field distribution, because there are no negative effects related to the reflection of waves from metal bars and the distribution is even.

Streszczenie: Celem niniejszej pracy jest analiza rozkładu pola elektromagnetycznego o częstotliwości f = 2.4 GHz wewnątrz pomieszczenia mieszkalnego. Analizie poddano wpływ materiału budowlanego i średnicy zbrojenia na rozkład

pola elektromagnetycznego. Do analizy wykorzystano metodę różnic skończonych w dziedzinie czasu (FDTD). Wyniki dowodzą, że montaż nadajników na ścianach bez zbrojenia powoduje równomierne rozłożenie pola elektromagnetycznego. Średnica prętów wpływa jedynie na rozkład pola i jego wartość tylko w odległości do 4 m. Szczegółowa analiza wpływu rodzaju konstrukcji budynku pozwoli rozwiązać problem zanikania. (Wpływ zbrojenia na rozkład natężenia pola elektrycznego).

Słowa kluczowe: bezprzewodowa komunikacja (Wi-Fi), propagacja fali elektromagnetycznej, materiały budowlane, FDTD.

Author: dr inż. Agnieszka Choroszucho, Bialystok University of Technology, Faculty of Electrical Engineering, Wiejska 45D, 15-351 Bialystok, E-mail: a.choroszucho@pb.edu.pl, ORCID: 0000-0001-7884-9264

This work was supported by the Ministry of Science and Higher Education in Poland at Bialystok University of Technology under research subsidy No. WZ/WE-IA/2/2020.

References

[1] Krzyżak, K. – Herko, E.: (2002) Symulacja propagacji fal radiowych we wnętrzu budynku, VII Konferencja Naukowo-Techniczna, ZKwE, pp. 207–210.

[2] Yee, K. S.: (1966) Numerical solution of initial boundary value problems Maxwell's equations in isotropic media. IEEE Transactions on Antennas and Propagation, vol. AP-14, No 3, pp. 302–307.

[3] Sikora, R.: (1997) Teoria pola elektromagnetycznego, Wydawnictwa Naukowo Techniczne, Warszawa.

[4] Taflove, A. – Hagness, S. C.: (2000) Computational electrodynamics. The finite – difference time – domain method. Boston, Artech House.

[5] Mur, G.: (1987) Absorbing boundary conditions for the finite – difference approximation of the time – domain electromagnetic field equations. IEEE Trans. on Biomed. Eng., Vol. BME-34, No. 2, pp. 148–157.

[6] QuickWave – 3D v.1.8, Warszawa, 1997.

[7] Polski Związek Inżynierów i Techników Budownictwa: (1985) Poradnik majstra budowlanego, Wydanie czwarte uzupełnione i rozszerzone, ARKADY, Warszawa.

[8] Praca zbiorowa: (1975) Poradnik laboranta budowlanego: Wydanie trzecie poprawione i uzupełnione, ARKADY, Warszawa.

[9] Taflove, A. – Brodwin, M. E.: (1975) Numerical solution of steady-state electromagnetic scattering problems using the time-dependent Maxwell's equitation. IEEE Trans. Microwave Theory Tech., MTT-23, 4, pp. 623–630.

[10] Morawski, T. – Gwarek, T.: (1998) Pola i fale elektromagnetyczne, WNT, Warszawa. ISBN 83-204-2238-8.

[11] Bogucki J.: (1994) Zasięg i poziomy promieniowania elektromagnetycznego, Przegląd Telekomunikacyjny, Rocznik LXXII, No. 1.

[12] Berenger, J. P.: (1994) A perfectly matched layer for the absorption of electromagnetic wave. J. Comput. Phys., vol. 114, 2, pp. 185–200.

[13] Duntemann, J.: (2006) Przewodnik po sieciach Wi-Fi. Nakom, Poznań.

[14] Machczyński, W.: (2004) Wprowadzenie do kompatybilności elektromagnetycznej. Wydawnictwo Politechniki Poznańskiej, Poznań.